Thermally Stable Sites for Electron Capture in Directly Ionized DNA: Free Radicals Produced by the Net Gain of Hydrogen at C5/C6 of Cytosine and Thymine in Crystalline Oligodeoxynucleotides

Michael G. Debije and William A. Bernhard*

Department of Biochemistry and Biophysics, University of Rochester, Rochester, New York 14642

Received: December 19, 2001; In Final Form: March 6, 2002

Electron paramagnetic resonance (EPR) spectroscopy is used to study radical trapping in crystalline oligodeoxynucleotides exposed to 70 keV x-irradiation at 4 K and annealed to 240 K. The four oligomers studied were the Z form d(CGCACG:GCGTGC), two A forms, $d(CCCTAGGG)_2$ and $d(GTGCGCAC)_2$, and the B form $d(CGCGAATTCGCG)_2$. In each of these oligomers, evidence was found for trapping of a cytosine radical formed by the net gain of a hydrogen at C_6 and a proton at N_3 (the $Cyt(C_6+H, N_3+H^+)^{+\bullet}$ radical). The data are consistent with the trapping of another cytosine radical formed by the net gain of hydrogen at C5 (the $Cyt(C_5+H, N_3+H)^{+\bullet}$ or $Cyt(C_5+H)^{\bullet}$ radical). The well-known thymine radical formed by the net gain of hydrogen at C5 ($Thy(C_6+H)^{\bullet}$ radical) was observed in the Z- and B-form duplexes but not in the A-form duplexes. The relative yields of these three reduction species indicate that cytosine is comparable to, or better than, thymine as a stable trapping site for reductive damage. These three radicals, $Cyt(C_6+H, N_3+H^+)^{+\bullet}$, $Cyt(C_5+H, N_3+H)^{+\bullet}$, and $Thy(C_6+H)^{\bullet}$, account for ∼85% of the total irreversibly trapped electrons in samples irradiated at 4 K and annealed to 240 K. Extrapolation of these results to B-form DNA hydrated to 9 waters per nucleotide, x-irradiated at 4 K, and warmed to room temperature predicts end product yields of 0.04−0.06 μmol/J for 5,6-dihydrouracil and 0.03−0.05 μmol/J for 5,6-dihydrothymine.

Introduction

Identification of the sites that trap holes and electrons in DNA is central to understanding the evolution of damage initiated in DNA by the direct effects of ionizing radiation. Direct-type effects consist of events generated by direct ionization of DNA and are derived from excess electrons and holes, some of which transfer into the helix from the hydration layer. These account for 30−50% of the stable damage produced in vivo.[1] The remaining 50−70% is due to reactions with radicals derived from water (primarily OH radicals), referred to as indirect-type effects. Radiation damage, indirect-type plus direct-type, is distributed in DNA nonhomogeneously, and it is this clustering of damage that makes living organisms highly sensitive to the effects of ionizing radiation.[2,3] The degree of clustering is a function of the mobility of electrons and holes and ultimately the location of stable trapping sites. There is, therefore, a keen interest in identifying those trapping sites that are thermally stable.

When DNA is irradiated at temperatures <77 K, a substantial fraction of the holes and electrons are stably trapped at that temperature. At these low temperatures, guanine is the major trapping site for holes,[4−6] whereas sugar radicals most likely account for the remaining fraction (∼30%).[7−9] For the excess electron, cytosine is the primary trapping site,[4,10−12] whereas thymine and adenine[10,11] are secondary sites. For DNA irradiated at <77 K, subsequent warming detraps and mobilizes a large fraction of holes and/or excess electrons, resulting in radical combination reactions and, thus, a decrease in total radical concentration.[13−16]

We have postulated previously that the initial step in detrapping of holes and electrons is the thermal activation of a reversible proton transfer.[13,17] Holes are stabilized at guanine by the transfer of a proton to N3 of cytosine from N1 of the guanine radical cation, giving the neutral $Gau(N1-H)^{\bullet}$ radical.[6,18] (See Figure 1 for structures and labels of the radicals discussed in this paper.) Back transfer of this same proton is thermally activated, consequently recreating the guanine radical cation. Holes in the form of the guanine radical cations may quickly tunnel to other guanines situated within about 1 nm.[13] Similarly, the excess electron is reversibly trapped by cytosine, with the extra stabilization coming from proton transfer to N3 of the cytosine radical anion from N1 of the base paired guanine.[6,13,17,18] Given sufficient thermal energy, this proton transfer is reversed, and thus, the gate for electron tunneling from the cytosine radical anion to nearby pyrimidines is opened. We refer to this thermally activated transfer as proton-gated hole/electron transfer. Once mobilized, the holes and excess electrons participate mainly in combination reactions, but a small fraction is irreversibly trapped.

Previous work suggested that the dominant site for irreversibly trapping the excess electron is thymine, occurring at temperatures above 130 K.[16,19−21] The key irreversible event is proton addition to C6 of the thymine radical anion, giving the neutral $Thy(C_6+H)^{\bullet}$ radical.[19−21] We noted recently in a study on electron trapping in $d(CGCG)_2$ crystals[22] that there are other reductive pathways that need to be explored. The $Cyt(C_6+H, N3+H)^{+\bullet}$ radical is formed at 4 K in $d(CGCG)_2$, and the concentration remains constant when the samples are annealed to 240 K. Because annealing to 240 K results in a 75% decrease

* To whom correspondence should be addressed: William A. Bernhard, Department Biochemistry/Biophysics, 575 Elmwood Ave., Rochester, NY 14642. E-mail: William_Bernhard@urmc.rochester.edu. Fax: (585) 275-6007. Phone: (585) 275-3730.

10.1021/jp014615+ CCC: $22.00
Published on Web 04/11/2002

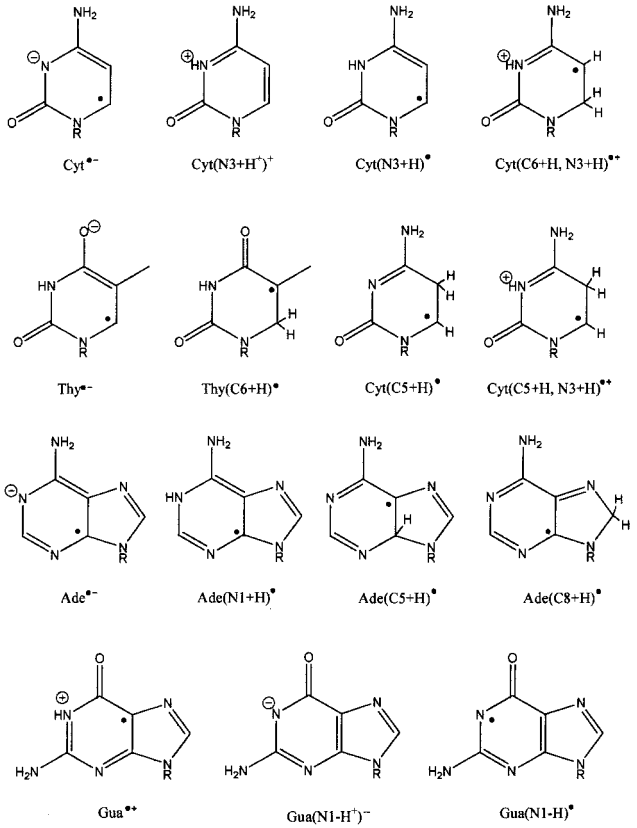

Figure 1. Structures of the radicals discussed in this work.

in the total radical concentration,[13,23] the relative amount of Cyt-(C_6+H, N3+H)$^{+\bullet}$ increases substantially: from 4% at 4 K to 10−15% at 240 K. Additionally, it was proposed that a closely related radical, Cyt(C_5+H, N_3+H)$^{+\bullet}$ (or Cyt(C_5+H)$^\bullet$), could be trapped in similar quantities and with the same properties of formation and annealing. In crystalline d(CGCG)$_2$, it was demonstrated that thermally mobilized holes and/or electrons do not significantly increase or decrease the radical population formed by pyrimidine reduction.

In the work presented here, we demonstrate that direct ionization produces the Cyt(C_6+H, N_3+H)$^{+\bullet}$ radical in crystalline DNA that contains thymine and adenine. The Cyt(C_6+H, N_3+H)$^{+\bullet}$ radical is formed at 4 K and persists upon annealing to 240 K. We show that the Thy(C_6+H)$^\bullet$ radical is formed in some samples and also infer the formation of the Cyt(C_5+H, N_3+H)$^{+\bullet}$ (or Cyt(C_5+H)$^\bullet$) radical. These three radicals combined account for about 85% of the reduced species in DNA. Cytosine appears to be the dominant site of irreversible reductive damage, equal to or exceeding that of thymine.

Materials and Methods

Crystals of four oligodeoxynucleotides, with sequences of d(CGCACG:GCGTGC),[24] d(CCCTAGGG)$_2$,[25] d(GTGCG-CAC)$_2$,[26] and d(CGCGAATTCGCG)$_2$,[27] were grown following published procedures from oligodeoxynucleotides purchased from Ransom Hill Bioscience (used without further purification). The level of DNA hydration, in mol H_2O/mol nucleotide, for each of these crystals was estimated to be 4.2, 9.3, 10.5, and 9.0, respectively.[28] The hexamer crystals formed continuously stacked Z-DNA. That is, the terminal base pair of one helix abutted the first base pair of the next helix, maintaining π-bond overlap. The d(CCCTAGGG)$_2$ and d(GTGCGCAC)$_2$ crystals grew quite large, but even single crystals gave powder-like EPR spectra owing to the space group and resulting large number of magnetically distinct trapping sites per unit cell. The packing of these oligodeoxynucleotides was such that the stacking within each A-form duplex was not continuous with any of the adjacent duplexes. The d(CGCGAATTCGCG)$_2$ crystals grew as hexagonal rods. The packing of this B-form duplex did not result in continuous base stacking between neighbor duplexes.

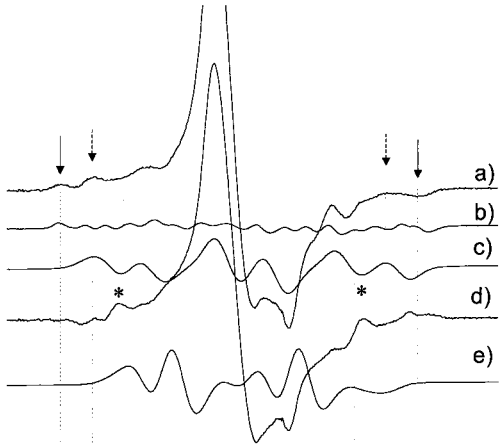

Figure 2. (a) EPR spectra of a 597 μg d(CGCGAATTCGCG)$_2$ polycrystalline sample irradiated to a dose of 20 kGy at 4K, then annealed to 240K, and returned to 4K for recording. (b) Spectrum of the Thy(C6+H)$^\bullet$ radical trapped in X irradiated dihydrothymine. (c) Simulated spectrum of Cyt(C6+H, N3+H$^+$)$^\bullet$. (d) Resultant spectrum after subtraction of spectra b and c from a. (e) Simulated spectrum of Cyt(C_5+H, N_3+H)$^{+\bullet}$. The solid arrows point to the outermost lines of the Thy(C_6+H)$^\bullet$ radical; the dashed arrows point to the outermost lines of the Cyt(C_6+H, N_3+H$^+$)$^{+\bullet}$ radical; and the asterisks indicate the outer lines of the presumed Cyt(C_5+H, N_3+H$^+$)$^{+\bullet}$ radical.

The single crystal of d(CGCACG:GCGTGC) was mounted with the long morphological axis perpendicular to an open Charles Supper quartz capillary (1.0 mm o.d.) using a small amount of rubber cement. Polycrystalline samples were sealed in Charles Supper quartz capillary tubes. Rotation of the single crystal was monitored by a goniometer attached to the top of the sample rod. The crystal was positioned so that at a goniometer angle of 90° ± 10° the *c* crystallographic axis was parallel to the external field $\mathbf{B}_0$. The 0° orientation places $\mathbf{B}_0$ in the plane of bases.

The samples were irradiated at 4 K to a dose of at least 15 kGy. The dose rate of 26 kGy/hr was provided by an OEG-76 tungsten filament X-ray tube maintained at a 70 keV and a current of 20 mA. The samples were raised into the EPR cavity and allowed to equilibrate for several minutes before spectra were recorded with a Q-band Varian E-12 spectrometer.[29]

Anneals were accomplished by raising the sample 40 cm above the cavity to the heater position, where the temperature was maintained to ±3% by a DRC-82 temperature controller from Lake Shore Cryotronics. The samples were kept at the annealing temperature for 10 minutes, then lowered back into the cavity and returned to 4 K before spectra were again recorded. Spectral simulations were performed using in-house software.[30,31]

Results

d(CGCGAATTCGCG)$_2$. An EPR spectrum of crystalline d(CGCGAATTCGCG)$_2$ exposed to x-irradiation at 4 K and annealed to 240 K is presented in Figure 2a. The outermost features, indicated by the solid arrows, are separated by about 14.2 mT. Of the radicals known to be formed in DNA and DNA constituents, there is only one that gives rise to a spectral width of this magnitude: the radical formed by the net gain of

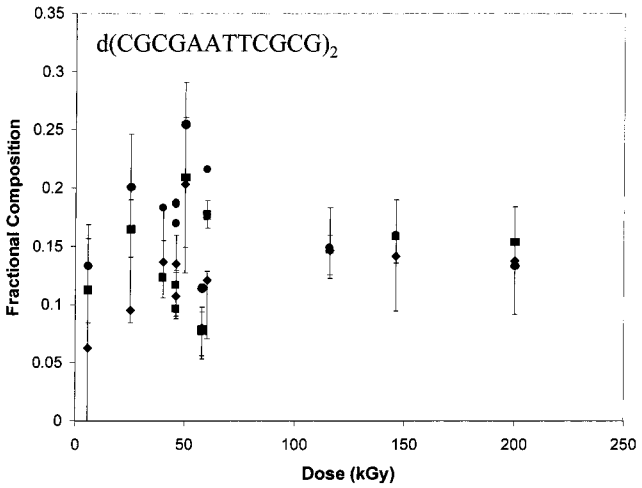

Figure 3. Fractional composition for specified radicals as a function of dose for crystalline d(CGCGAATTCGCG)$_2$ annealed to 240 K: diamonds, [Thy(C$_6$+H)$^\bullet$ radical]/[total radicals]; squares, [Cyt(C$_6$+H, N$_3$+H$^+$)$^{+\bullet}$]/[total radicals]; and circles, [Cyt(C$_5$+H, N$_3$+H$^+$)$^{+\bullet}$]/[total radicals].

hydrogen at C$_6$ of thymine. The structure of the Thy(C$_6$+H)$^\bullet$ radical is shown in Figure 1. The separation between the outermost lines (spectral width) of Thy(C$_6$+H)$^\bullet$ has been measured in various thymine derivatives to be 13.6−14.2 mT.[32−35] In irradiated DNA at 4 K, identifying features of the Thy(C$_6$+H)$^\bullet$ are limited to the outermost lines for the reasons described below.

A reference spectrum of the Thy(C$_6$+H)$^\bullet$ radical, shown in Figure 2b, is taken from an earlier study.[36] This relatively pure spectrum was obtained by x-irradiating dihydrothymine at ∼23 °C, annealing to 100 °C, and recording the spectrum at 4 K at Q-band microwave frequencies. The spectrum differs from that of the well-known 1:3:5:7:7:5:3:1 octet that is observed at temperatures above ∼50 K. The octet pattern comes from the equivalency of the three methyl hydrogen couplings, and the coincidence that the methyl splitting is about $^1/_2$ the splitting of the two (roughly) equivalent methylene hydrogens. At 4 K, the methyl rotation slows substantially, making the methyl hydrogens nonequivalent.[37] Also, the difference between the methylene hydrogen couplings is larger when the radical is derived from dihydrothymine as opposed to thymine. Thus, the reference spectrum at 4 K shows 16 resolved lines (out of a potential 32) with relative intensities between 1:1 and 1:2. In comparing the reference spectrum to that of a Thy(C$_6$+H)$^\bullet$ radical trapped in the oligomer, it is also important to note that thymines at different oligomer positions may give different sets of beta hydrogen couplings because these couplings are very sensitive to the nonplanarity of the pyrimidine ring. Although these factors make the multiplicity, intensity pattern, and line widths variable, the spectral width of Thy(C$_6$+H)$^\bullet$ in DNA should not vary, and in fact, it does compare well with that of the reference spectrum.

The relative concentration of Thy(C$_6$+H)$^\bullet$ radical in the crystalline oligodeoxynucleotides is measured by fitting the outermost features of the reference spectrum to those of the experimental spectrum and then comparing the intensities of these two spectra. The ratio, [Thy(C$_6$+H)$^\bullet$ radical]/[total radicals], is plotted as a function of dose in Figure 3 (solid diamonds). (The total radical yield for crystalline d(CGCGAATTCGCG)$_2$ is 0.66 ± 0.06 μmol/J.[23]) These measurements, the average from six samples, indicate that for doses >20 kGy the thymine radical concentration, [Thy(C$_6$+H)$^\bullet$], is ∼13% of the total radical concentration, [total radicals]. Assuming that half of the total radicals is produced through a reductive

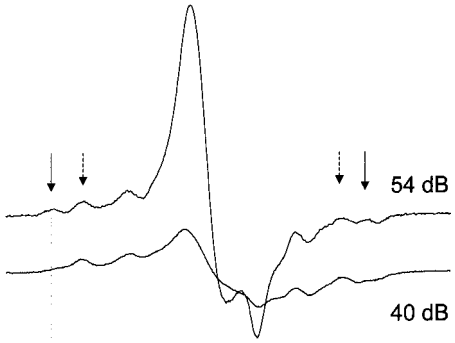

Figure 4. Power saturation study of crystalline d(CGCGAATTCGCG)$_2$ irradiated at 4 K and annealed to 240 K. EPR spectrum taken at 4 K using a microwave power attenuation of (a) 54 dB and (b) 40 dB (at 0 dB the power is 25 mW). The solid arrows point to the outermost lines of the Thy(C$_6$+H)$^\bullet$ radical, and the dashed arrows point to the outermost lines of the Cyt(C$_6$+H, N$_3$+H$^+$)$^{+\bullet}$ radical.

pathway, Thy(C$_6$+H)$^\bullet$ accounts for ∼26% of the reduction generated radicals. If all such radicals end up on the pyrimidines, and the probability of radical trapping by thymine equals that of cytosine, we expect Thy(C$_6$+H)$^\bullet$ to account for 33% of the reduction radicals (2 thymines/6 pyrimidines). In other words, these assumptions lead to the prediction that 16% of all the trapped radicals should be due to reduced thymine. On the basis of the observed value of ∼13%, the probability of one-electron reduction of thymine is comparable to that of cytosine when the oligomer duplex is irradiated at 4 K and annealed to 240 K.

It can be seen from Figure 4 that upon increasing the microwave power the signal assigned to Thy(C$_6$+H)$^\bullet$ is broadened because of power saturation, whereas the adjacent lines are not. This suggests that the adjacent lines belong to other radicals with different power saturation characteristics. The two outer lines that do not power saturate are separated by ∼11.6 mT. This spectral width is diagnostic for the Cyt(C$_6$+H, N$_3$+H$^+$)$^{+\bullet}$ radical.[22] The simulated spectrum of Cyt(C$_6$+H, N$_3$+H$^+$)$^{+\bullet}$ using the parameters described in the pervious work[22] is presented as Figure 2c. The fractional content of Cyt(C$_6$+H, N$_3$+H)$^{+\bullet}$ was determined by comparing the simulated spectrum to the experimental spectrum after subtraction of the Thy-(C6+H)$^\bullet$ reference spectrum. The fractional concentration of Cyt(C$_6$+H, N$_3$+H$^+$)$^{+\bullet}$ is plotted as solid squares in Figure 3. At higher doses, this radical makes up ∼14% of the total radical population or ∼28% of the reduced species. The fractional concentration, [Cyt(C$_6$+H, N$_3$+H$^+$)$^{+\bullet}$]/[total radicals], as a function of annealing temperature is plotted as solid squares in Figure 5. Note that the absolute population of the radical (open squares) does not change as the sample is warmed from 4 to 240 K. This suggests that the Cyt(C$_6$+H, N$_3$+H$^+$)$^{+\bullet}$ radical is formed at 4 K and does not decay upon annealing, nor is there an electron transfer to cytosine which subsequently promotes the formation of this irreversibly trapped radical at higher temperatures. The same observations apply to the Thy(C$_6$+H)$^\bullet$ radical as can be seen from the data in Figure 5.

Subtraction of the spectra of both Thy(C$_6$+H)$^\bullet$ and Cyt-(C$_6$+H, N$_3$+H$^+$)$^\bullet$ from the experimental d(CGCGAATTCGCG)$_2$ spectrum yields the resultant shown in Figure 2d. The two outermost features of the spectrum in Figure 2d, marked by asterisks, have a separation of roughly 9.5 mT. Such features, revealed after subtracting two other components, are difficult to use a priori in making a free radical assignment. However, a spectral component having a 9.5 mT width is consistent with the presence of the Cyt(C$_5$+H, N$_3$+H)$^{+\bullet}$/Cyt(C$_5$+H)$^\bullet$ radical.[22,38,39] (The spectral width does not distinguish between the Cyt(C$_5$+H)$^\bullet$ radical and its N$_3$ protonated form, Cyt(C$_5$+H,

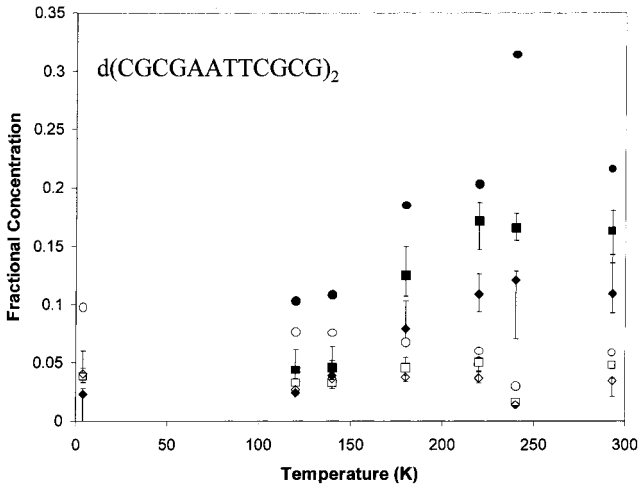

Figure 5. Fractional composition for the three radicals as a function of annealing temperature in $d(CGCGAATTCGCG)_2$ irradiated to a dose of 20 kGy at 4 K, annealed to the temperature shown, and returned to 4 K for recording. The solid symbols are for the concentration of a specific radical relative to the concentration of total radical remaining after annealing to a given temperature. The open symbols are for the concentration of a specific radical relative to the concentration of total radicals observed at 4 K prior to any annealing. The symbols relate to the following radicals: diamonds, Thy(C_6+H)$^\bullet$ radical; squares, Cyt(C_6+H, N_3+H^+)$^{+\bullet}$; and circles, Cyt(C_5+H, N_3+H^+)$^{+\bullet}$.

N_3+H)$^{+\bullet}$.) The only other radicals that would present a spectrum with this width are sugar radicals (either H abstraction from $C_{2'}$ or $C_{3'}$).[7] However, as argued previously,[22] a 1:1 stoichiometry of radicals generated by reduction vs oxidation favors the presence of Cyt(C_5+H, N_3+H)$^{+\bullet}$. Using a spectral simulation of Cyt(C_5+H, N_3+H)$^{+\bullet}$ (shown in Figure 2e), we estimate the remaining concentration of this radical species to be about 16% of the total radical concentration after doses >20 kGy and annealing to 240 K.

These three radicals, Thy(C_6+H)$^\bullet$, Cyt(C_6+H, N_3+H^+)$^\bullet$, and Cyt(C_5+H, N_3+H)$^{+\bullet}$, may account for ~85% of the reduced species in $d(CGCGAATTCGCG)_2$ irradiated at 4 K and annealed to 240 K. Although the relative fractions of each radical species are somewhat dependent on dose (Figure 3), reduction of cytosine consistently exceeds reduction of thymine. In terms of free radical yields, the sum of cytosine H-adduct radicals (C(C5,6+H)$^\bullet$) is 0.05−0.08 μmol/J and Thy(C_6+H)$^\bullet$ is 0.02−0.03 μmol/J.

d(CGCACG:GCGTGC). EPR spectra for d(CGCACG:GCGTGC) are presented in Figure 6. The spectra are for a single-crystal irradiated to 17 kGy at 4 K, annealed to 240 K, returned to 4 K, and rotated about an axis lying in the *ab* plane such that at 0° the external field $\mathbf{B}_0$ is perpendicular to the helical axis and parallel to the base planes. The spectrum of Thy(C_6+H)$^\bullet$ is not detected until reaching doses between 25 and 50 kGy. The [Thy(C_6+H)$^\bullet$]/[total radical] fraction, after 240 K anneal, is 3−5%. Assuming that half the radicals are produced by reduction, that radicals produced by reduction are trapped selectively by pyrimidines, and that trapping by thymine and cytosine is equally probable and given the ratio of one thymine per six pyrimidines, one predicts that 17% of the total radicals should be Thy(C_6+H)$^\bullet$. Because the observed fraction is less than predicted, there is the possibility that irreversible trapping by thymine is less efficient than by cytosine. There are weak outer lines, indicated in Figure 6 by dashed arrows, that are separated by ~11.6 mT. These features are assigned to the Cyt(C_6+H, N_3+H^+)$^{+\bullet}$ radical. In three crystalline samples irradiated to 26 kGy, the concentration of Cyt(C_6+H, N_3+H^+)$^{+\bullet}$ after 240 K anneal was determined using the same procedure as above. The ratio of [Cyt(C_6+H, N_3+H^+)$^{+\bullet}$]/[total radicals] is ~8−10% (16−20% of the reduction produced radicals).

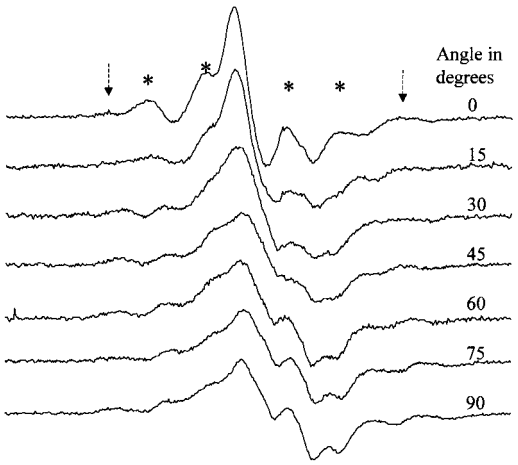

Figure 6. EPR spectra of a single crystal of d(CGCACG:GCGTGC) rotated about the *a*/*b* axis (exact orientation not known) after a 17 kGy irradiation at 4 K, annealing to 240 K, and returning to 4 K. 0° is defined as the orientation wherein the base planes of the crystal are oriented parallel to the external field (that is, the *c* axis, or long axis of the crystal corresponding to the helical axis, is perpendicular to $\mathbf{B}_0$). Rotations were in increments of 15°. The field center is 126.0 mT, and the scan width is 20 mT. The dashed arrows point to the outermost lines of the Cyt(C_6+H, N_3+H^+)$^{+\bullet}$ radical, and the asterisks indicate four of the lines attributed to the Cyt(C_5+H, N_3+H^+)$^{+\bullet}$ radical.

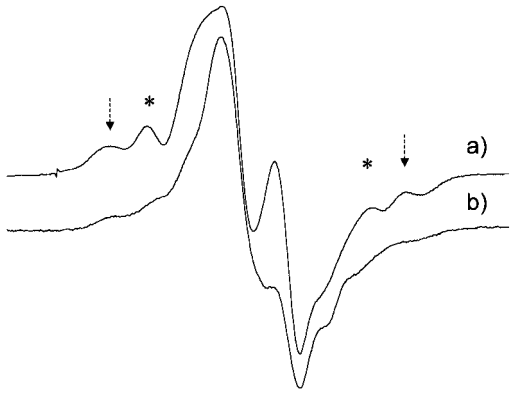

Figure 7. EPR spectra of (a) 741 μg polycrystalline $d(CCCTAGGG)_2$ annealed to 240 K after being irradiated to a dose of 52 kGy at 4 K and (b) 731 μg polycrystalline $d(GTGCGCAC)_2$ annealed to 240 K after being irradiated to a dose of 39 kGy at 4 K. The dashed arrows point to the outermost lines of the Cyt(C_6+H, N_3+H^+)$^{+\bullet}$ radical, and the asterisks indicate the outer lines of the presumed Cyt(C_5+H, N_3+H^+)$^{+\bullet}$ radical.

The concentration of the presumed Cyt(C_5+H, N_3+H)$^{+\bullet}$ radical was estimated for the hexamer samples using the procedure described for $d(CGCGAATTCGCG)_2$. The ratio of [Cyt(C_5+H, N_3+H)$^{+\bullet}$]/[total radicals] is 18−25% (36−50% of the reduction produced radicals). In total, 60−80% of the reduced species in the DNA crystalline sample can be accounted for by these three radicals. The yield for the sum of cytosine H-adduct radicals (C(C5,6+H)$^\bullet$) is 0.04−0.09 μmol/J, and the yield of Thy(C_6+H)$^\bullet$ is 0.005−0.01 μmol/J.

$d(CCCTAGGG)_2$ and $d(GTGCGCAC)_2$ Crystals. The EPR spectrum for crystals of the octamers $d(CCCTAGGG)_2$ and $d(GTGCGCAC)_2$ are shown in Figure 7 parts a and b. The outermost lines, indicated by the dashed arrows, are split by 11.8 mT and are assigned to the Cyt(C_6+H, N_3+H^+)$^{+\bullet}$ radical. The next pair of lines, indicated by asterisks, fall at the outer

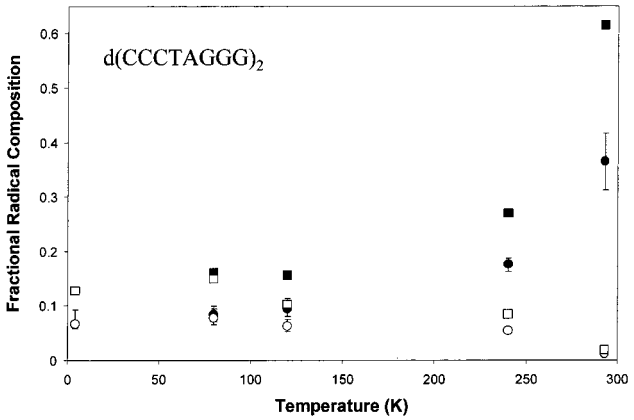

Figure 8. Fractional composition for the three radicals as a function of annealing temperature in $d(CCCTAGGG)_2$ irradiated to a dose of 21 kGy at 4 K, annealed to 240 K, and returned to 4 K for recording. The solid symbols are for the concentration of a specific radical relative to the concentration of total radical remaining after annealing to a given temperature. The open symbols are for the concentration of a specific radical relative to the concentration of total radicals observed at 4 K prior to any annealing. The symbols relate to the following radicals: squares, Cyt(C_6+H, N_3+H^+)$^{+\bullet}$; circles, Cyt(C_5+H, N_3+H^+)$^{+\bullet}$.

extent of the Cyt(C_5+H, N_3+H)$^{+\bullet}$ radical, ~9.0 mT. The difference in line width (spectral resolution) is due to one large crystal being used as a sample in Figure 7a and a polycrystalline sample used in Figure 7b. There is an absence of the features assigned to the Thy(C_6+H)$^\bullet$ radical, and this holds true even at doses high enough to easily recognize these features in the other crystals. Using the same procedure as above, 15% of the total radical population in $d(CCCTAGGG)_2$ (irradiated to a dose >21 kGy and annealed to 240 K) is due to the Cyt(C_6+H, N_3+H^+)$^\bullet$ radical, and about 20% is due to the assumed Cyt(C_5+H, N_3+H)$^{+\bullet}$ radical. As may be seen in Figure 8, the Cyt(C_6+H, N_3+H^+)$^{+\bullet}$ radical is formed at 4 K, and its relative concentration increases upon annealing. However, its absolute concentration remains constant up to 240 K and then drops upon annealing to room temperature. The same is true for the Cyt(C_5+H, N_3+H)$^{+\bullet}$ radical. The concentration of Thy(C_6+H)$^\bullet$ is below the detection limit, which is about 2% of the total radical concentration. The yield for the sum of cytosine H-adduct radicals (C(C5,6+H)$^\bullet$) is 0.02−0.09 μmol/J.

In $d(GTGCGCAC)_2$ samples, treated the same as the $d(CCCTAGGG)_2$ crystals, the ratio of [Cyt(C_6+H, N_3+H^+)$^{+\bullet}$]/[total radicals] is 11% and the ratio of [Cyt(C_5+H, N_3+H)$^{+\bullet}$]/[total radicals] is ~18%. The spectral signature of the Thy(C_6+H)$^\bullet$ radical is not observed. The yield for the sum of cytosine H-adduct radicals (C(C5,6+H)$^\bullet$) is 0.06−0.08 μmol/J.

Discussion

Free radicals, stable up to 240 K, are trapped by cytosine and thymine through the net gain of hydrogen at C_5 and/or C_6. Two of these radicals, Cyt(C_6+H, N_3+H^+)$^{+\bullet}$ and Thy(C_6+H)$^\bullet$, are identified with a high confidence level because of the large and distinctive width of their EPR spectra. Evidence for the Cyt(C_5+H, N_3+H)$^{+\bullet}$/Cyt(C_5+H)$^\bullet$ radical is not as strong, but now that spectral lines consistent with its presence have been observed in five different crystals, the confidence level has increased. The concentration of these three radicals, relative to the total radical concentration, [R_t], is summarized in Table 1 along with information on DNA conformation, continuity of stacking, 4 K yield of R_t, and fraction of radicals remaining after annealing to 240 K. In the last three columns, the ratio between [Thy(C_6+H)$^\bullet$] and [Cyt(C_6+H, N_3+H^+)$^{+\bullet}$]+[Cyt-(C_5+H, N_3+H)$^{+\bullet}$] (designated [T+H]:[C+H]) is seen to conform closely to the Thy:Cyt ratio for the Z- and B-form duplexes but not the two A-form duplexes. Normalizing for the relative abundance of thymine verses cytosine, the probability of trapping by thymine (T_{prob}) is compared with trapping by cytosine (C_{prob}). In all four oligomer duplexes, the probability of irreversible trapping by cytosine is greater.

If one assumes that the cytosine H-adduct radicals lead to the stable end product of 5,6-dihydrouracil[40] with a stoichiometry of 1:1, then the yield of these products for B-DNA, with a AT/CG ratio of 1.0 and hydrated to 9 waters/nucleotide, is predicted to be 0.04−0.06 μmol/J. Similarly, the yield of 5,6-dihydrothymine is predicted to be 0.03−0.05 μmol/J. These predicted yields are remarkably close to those measured by Steven G. Swarts for vacuum-dried salmon-sperm DNA, hydrated under N_2 to 10.3 waters nucleotide (personal communication). For 5,6-dihydrouracil and 5,6-dihydrothymine, Swarts obtained 0.04 ± 0.01 and 0.07 ± 0.2 μmol/J, respectively. Unlike our projection (based on crystalline DNA irradiated at 4 K), the dihydrothymine yield is the larger of the two.

It is notable that the two A form oligodeoxynucleotides give very little, if any, radical trapping by thymine. A possibility is that the tighter base stacking of the A form (0.27 nm), compared to the B (0.34 nm) and Z forms (0.37 nm), hinders H addition in thymine but not cytosine. Another possibility is that the spectrum of the Thy(C_6+H)$^\bullet$ radical is more difficult to detect in A-form DNA. This could arise if the five β-hydrogen couplings are all sufficiently different[41] so as give very poor resolution. We also note that in all four duplexes, about $^1/_3$ of all of the radicals stable at 240 K appear to be radicals produced by the reduction of cytosine.

To explain these findings, a working model is outlined in Figure 9. A major assumption of the model is that half of the radicals trapped at 4 K are derived from one-electron loss (hole formation) and that the other half are derived from one-electron gain; it is assumed, therefore, that no radicals are derived via hydrogen atom abstraction or addition. The events modeled are those occurring after the electrons and holes have settled out on the DNA: that is, the thermalized electrons have been captured by the bases and the holes initially formed in tightly

TABLE 1: Relative Efficiencies of Irreversible Radical Trapping by Thymine vs Cytosine in Oligodeoxynucleotide Duplexes[a]

sequence	form/ stack	yield of R_t at 4 K[b] (μmol/J)	$[R_t]_{240K} \div [R_t]_{4K}$	$[C_{C6+H}] \div [R_t]_{240K}$	$[C_{C5+H}] \div [R_t]_{240K}$	$[T_{C5+H}] \div [R_t]_{240K}$	[Thy] ÷ [Cyt]	$[T_{C5+H}] \div$ [C+H]	$T_{prob} \div C_{prob}$
$d(CGCG)_2$	Z/y	0.65 ± 0.15	0.10−0.33	~0.12	~0.22	na	na	na	na
d(CGCACG:GCGTGC)	Z/y	~0.7[c]	0.19−0.42	~0.09	~0.22	~0.04	1:5	1:7.8	1:1.6
$d(CGCGAATTCGCG)_2$	B/n	0.66 ± 0.06	0.24−0.40	~0.14	~0.16	~0.13	1:2	1:2.3	1:1.2
$d(CCCTAGGG)_2$	A/n	0.70 ± 0.04	0.09−0.35	~0.15	~0.20	<0.02	1:3	<1:18	<1:6
$d(GTGCGCAC)_2$	A/n	0.72 ± 0.07	0.30−0.39	~0.11	~0.18	<0.02	1:3	<1:15	<1:5

[a] Column headings are: form ≡ duplex form/stack ≡ continuity in base stacking; [Rt]≡[total radicals]; $[C_{C6+H}]$≡ [Cyt(C_6+H, N_3+H^+)$^{+\bullet}$]; $[C_{C5+H}]$≡[Cyt(C_5+H, N_3+H^+)$^{+\bullet}$]; $[T_{C5+H}]$≡[Thy(C_6+H)$^\bullet$]; [C+H]≡$[C_{C6+H}]$ + $[C_{C5+H}]$; $T_{prob} \div C_{prob}$ is the probability of irreversible trapping by thymine relative to cytosine. [b] Reference 23. [c] Estimated yield. The yield determination is complicated by the presence of an unknown quantity of barium within the crystal.

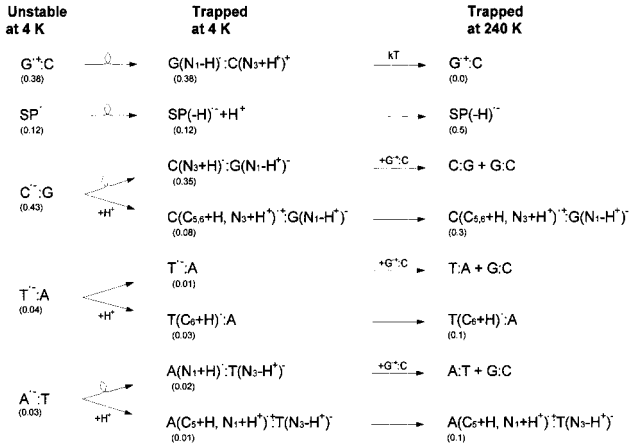

Figure 9. Model proposed to explain the evolution of damage in crystalline oligodeoxynucleotide duplexes. Three stages are shown: left column, sites of hole and electron attachment after thermalization but before stabilization at 4 K; middle column, stably trapped radicals at 4 K; right column, final trapping sites after annealing to 240 K.

bound water have transferred to DNA. The five starting radicals are then $G^{+\bullet}$:C (guanine radical cation), $SP^{\bullet}$ (sugar phosphate radical), $C^{-\bullet}$:G (cytosine radical anion), $T^{-\bullet}$:A (thymine radical anion), and $A^{-\bullet}$:T (adenine radical anion) with relative concentrations of 0.38:0.12:0.43:0.04:0.03, respectively.[10] These radicals, with the possible exception of $T^{-\bullet}$:A, are unstable at 4 K and are not observed. Reversible proton transfer, across the Watson−Crick hydrogen bond, stabilizes the hole at G and the excess electron at C and A.[42] It is less clear whether reversible proton-transfer stabilizes the electron on T, which would give the Thy(O_4+H)$^{\bullet}$ radical.[43−45] For simplicity, we assume it does not. Irreversible deprotonation from the sugar phosphate backbone traps out a family of radicals formed by the net loss of hydrogen from each of the five deoxyribose carbons. (Collectively designated SP(−H)$^{-\bullet}$, the parent sugar phosphate anion, having lost one electron and one proton, is a radical anion.) The protons released by ionization of SP directly (or indirectly) promote proton addition to carbon sites of the base radical anions, yielding base radicals that are irreversibly protonated. In the second column of Figure 9, the radicals are trapped by reversible and irreversible protonation and are stable indefinitely at 4 K.

The radical concentration, upon warming to 240 K, decreases more or less monotonically.[13] We have previously suggested that this was due to detrapping of either the hole and/or the electron, where back transfer of the proton creates the mobile $G^{+\bullet}$ and $C^{-\bullet}$ species.[17] For reasons explained below, we now prefer a model where primarily the hole is detrapped under these conditions. Thus, $G^{+\bullet}$ is mobilized, and it undergoes a random three-dimensional walk through the crystal by tunneling to nearby guanines (intrastrand, interstrand, and intermolecular).[13] Given sufficient thermal energy, the hole continues its walk until irreversibly trapped by OH^- addition[46] or by recombining with another radical. Under our annealing conditions, we presume that the latter predominates. In addition, it is assumed that the probability of recombining with one of the three reversibly protonated reduced bases is large and that the probability of recombining with one of the irreversibly protonated/deprotonated radicals is small. By this scheme, one is left with a population, after 240 K anneal, that contains radicals that are due to H addition to C_5-C_6 of cytosine, H addition to C_5 of thymine, H addition to C_5/C_8 of adenine, and H abstraction from sugar. The relative concentrations of these are approximately 0.3:0.1:0.1:0.5, respectively. Evidence for the first two radical types is given here; evidence for the third is a mater of conjecture based on work on reduction of adenine in monomeric and oligomeric systems,[10,47−49] and evidence for the fourth comes from the yields of end products[9,50] related to sugar damage.

The relative probabilities (concentrations) given in our model were rationalized as follows. For the one-electron reduction side, we used the distribution for electron attachment observed for oligomer duplexes in LiCl glasses.[10] In that work, it was found that 87% of electron capture is by C and the remaining 13% is split between T and A, giving the ratio of 0.43:0.04:0.03 for $[C^{-\bullet}]:[T^{-\bullet}]:[A^{-\bullet}]$. Next, the measured fraction of cytosine C_5-C_6 adduct at 4 K in d(CGCGAATTCGCG)$_2$ was used to split the $C^{-\bullet}$ into 0.35 of $C(N_3+H)^{\bullet}:G(N_1-H^+)^-$ and 0.08 of $C(C_{5,6}+H, N_3+H^+)^{+\bullet}:G(N_1-H^+)^-$. In the same way, $T^{-\bullet}$ was split into 0.01 of $T^{-\bullet}$:A and 0.03 of $T(C_5+H)^{\bullet}$:A. The relative value of $[A^{-\bullet}]$ is an educated guess. The fraction assigned to sugar radicals is based on the strand break yields determined for a series of crystalline oligodeoxynucleotides where that yield corresponds to 10−15% of the radical yields in those oligomers.[9,50] Also, because the sugar is the presumed source of protons (directly or indirectly) for the three pyrimidines radicals formed by protonation at carbon, the fraction of $SP^{\bullet}$ is constrained to $\geq(0.08 + 0.03 + 0.01)$. The remaining fraction of the holes, 0.38, was by default attached to guanine. Starting with these relative probabilities for the distribution of radicals at 4 K, the distribution at 240 K follows from the model. In this model, the underlying evidence for the mechanisms is more persuasive than the precise ratios of radical intermediates. The ratios appear to vary by sample type, pointing to the possible importance of crystal lattice structure and DNA confirmation.

The model is consistent with the fraction of radicals lost (ΔR_t) upon annealing from 4 to 240 K. ΔR_t must be less than or equal to either $2[G^{+\bullet}]$ or $2\{[C(N_3+H)^{\bullet}:G(N_1-H^+)^-]+[T^{-\bullet}:A]+[A(N_1+H)^{\bullet}:T(N_3-H^+)^-]\}$, whichever is smaller. The former is a consequence of the assumption that the only one-electron oxidized species participating in combination reactions is $G^{+\bullet}$, not SP(−H)$^{-\bullet}$, and that the number of radicals lost is maximized if all $G^{+\bullet}$ radicals react with one-electron reduction sites. The later applies the corresponding assumptions to the mobile one-electron reduction species: $C(N_3+H)^{\bullet}:G(N_1-H^+)^-$, $T^{-\bullet}$:A, plus $A(N_1+H)^{\bullet}:T(N_3-H^+)^-$. For the fractions given in the model, these two quantities are the same and result in a $\Delta R_t \geq 76\%$.

The proposal that holes are detrapped at temperatures that are lower than the temperatures required to detrap the excess electrons is based on the following reasoning. The pK_a measurements on monomer systems by Steenken[42,51] predict an equilibrium of $K = 10^{0.4}$, favoring the proton at the N_3 position of cytosine for the hole localized on G of a C:G pair. Furthermore, for electron capture by C in a C:G pair, Steenken predicted an equilibrium of $K \geq 10^{3.5}$. From these predictions, hole formation at G favors deprotonation across the $G(N_1)-C(N_3)$ hydrogen bond by 2.3 kJ. Similarly, for the electron adduct at C, protonation of C via the $G(N_1)-C(N_3)$ hydrogen bond is favored by 20 kJ. Ab initio, molecular orbital calculations on the change in free energy associated with proton transfer are in excellent agreement with both of these values.[52,53] On the basis of thermodynamics, therefore, one expects that the activation energy needed to detrap the hole from G in duplex DNA is relatively small, an order of magnitude less than that needed to detrap the electron. This fits quite well with the observation that, upon warming 4 K irradiated crystalline DNA to 77 K, 10−30% of the radicals anneal out, i.e., at least one of the trapping sites (vide infra $G^{+\bullet}$) is very shallow.

What about detrapping of the excess electron from thymine and adenine, both of which are more shallow than cytosine?[4,20] Once detrapped, the most likely fate of these electrons is to be retrapped by cytosine.[10] For amorphous DNA irradiated at 77 K, the radical concentration undergoes most of its decline between 160 and 220 K and [Thy(C_5+H)$^\bullet$] increases between 140 and 190 K.[19] In contrast, for crystalline DNA irradiated at 4 K, we do not see any change in the concentration of carbon H adducts of thymine or cytosine over this temperature range. This suggests that the precursor radicals, $T^{-\bullet}$:A and C(N_3+H)$^\bullet$:G(N_1-H^+)$^-$, are depleted before reaching the temperature range that activates carbon protonation. We suggest, therefore, that the decrease in radical concentration that occurs in 4 K irradiated crystalline DNA between 4 and roughly 160 K is predominantly a consequence of hole mobility. Because hole transfer is gated by proton transfer and the activation energy for proton transfer has a large dispersion, the annealing profile is relatively monotonic.[13]

It is important to reconcile the findings reported here and our working model with observations made by Sevilla and coworkers on high molecular weight DNA γ-irradiated at 77 K.[19,54] They find that the T(C_5+H)$^\bullet$ radical concentration increases between 140 and 190 K at the expense of the C(N_3+H)$^\bullet$ radical concentration. Their proposed mechanism is based on the reactions

$$C(N_3+H)^\bullet \underset{\pm\mathbf{1}}{\longleftrightarrow} C^{-\bullet} \underset{\pm\mathbf{2}}{\longleftrightarrow} T^{-\bullet} \underset{\mathbf{3}}{\rightarrow} T(C_5+H)^\bullet$$

where +**1** is thermally activated above ~140 K, mobilizing the excess electron. Reaction **3** is thermally activated in the same temperature range, trapping the excess electron by irreversible protonation at C5 of thymine. Our results and model do not support or refute this. In crystalline DNA, the population of shallow trapped electrons appears to be significantly depleted once the temperature needed to activate reaction **3** is reached. Under these circumstance, there remains no source of excess electrons; that is, Thy$^{\bullet-}$ and Cyt(N_3+H)$^\bullet$ are depleted or at least below our limit of detecting an increase in [T(C_5+H)$^\bullet$] or [Cyt(C_6+H, N_3+H^+)$^{+\bullet}$]. That limit is on the order of ±5% of the radical concentration at 4 K. Although depletion of Thy$^{\bullet-}$ and Cyt(N_3+H)$^\bullet$ is a plausible explanation, other questions remain. For example, how does the temperature of irradiation (4 vs 77 K) affect the temperature dependence for depletion of reversibly trapped holes and electrons? This and other questions need to be answered by considering the list of differences between these two experiments: (1) the DNA molecular weight and packing are substantially different, (2) the hydration states are different, (3) the radiation quality is a bit different (70 KV X-rays vs γ-rays), and (4) there are differences in base composition and DNA conformation. Consider, for example, that, during DNA irradiation at 77 K, 10−30% more radicals are lost to combination reactions than when irradiated at 4 K. The absolute yield of radicals in crystals (x-irradiated at 4 K and annealed to 77 K) is nearly twice that of amorphous DNA.[23,55] This may introduce substantial differences in spatial distribution and subsequent probabilities of radical combination reactions. Also, in frozen DNA solutions, it has been concluded that the ratio of electron adducts to trapped holes is ~0.6:0.4, with the net excess in attached electrons being balanced by holes trapped in the bulk water (ice).[54] Under such conditions, at least 30% of the initially trapped electrons could not readily combine with a hole, and furthermore, the bulk ice should contain a matching amount of hydronium ions. In frozen DNA solutions, this provides a platform for reactions **1**−**3**, a platform that probably does not exist in crystalline DNA. This could also explain the observation by Swarts (cited above), in which the end product yields of 5,6-dihydrothymine are larger than the yield of 5,6-dihydrocytosine.

Conclusions

Irreversible electron trapping by cytosine is favorable in crystalline oligodeoxynucleotide duplexes irradiated at 4 K. Trapping by cytosine is equivalent to, or more favorable than, that by thymine as judged by the yields of radicals produced by the net gain of hydrogen at C_6 and C_5 of cytosine relative to the yield of radicals formed by the net gain of hydrogen at C_5 of thymine. The three reduced species Cyt(C_6+H, N_3+H^+)$^\bullet$, Cyt(C_5+H, N_3+H)$^{+\bullet}$, and Thy(C_5+H)$^\bullet$ account for about 85% of the reduction generated radicals that remain stable after annealing 4 K irradiated DNA to 240 K. For B-DNA with a AT/CG ratio of 1.0, these results predict a yield of 5,6-dihydrouracil of 0.04−0.06 μmol/J and a yield of 5,6-dihydrothymine of 0.03−0.05 μmol/J.

Acknowledgment. For invaluable technical assistance, the authors thank Kermit R. Mercer, and for critically reading the manuscript, we thank Yuriy Razskazovskiy, Shubhadeep Purkaystha, David Gilbert, and Steve Swarts. This study was supported by PHS Grant 2-R01-CA32546, awarded by the National Cancer Institute. Its contents are solely the responsibility of the authors and do not necessarily represent the official views of the NCI.

References and Notes

(1) Krisch, R. E.; Flick, M. B.; Trumbore, C. N. *Radiat. Res.* **1991**, *126*, 251−259.
(2) Ward, J. F. *Radiat. Res.* **1981**, *86*, 185−95.
(3) Goodhead, D. T. *Int. J. Radiat. Biol* **1994**, *65*, 7−17.
(4) Sevilla, M. D.; Becker, D.; Yan, M.; Summerfield, S. *J. Phys. Chem.* **1991**, *95*, 3409−15.
(5) Close, D. M. *Radiat. Res.* **1993**, *135*, 1−15.
(6) Steenken, S.; Jovanovic, S. V. *J. Am. Chem. Soc.* **1997**, *119*, 617−618.
(7) Close, D. M. *Radiat. Res.* **1997**, *147*, 663−673.
(8) Debije, M. G.; Bernhard, W. A. *Radiat. Res.* **2001**, *155*, 687−692.
(9) Debije, M. G.; Razskazovskiy, Y.; Bernhard, W. A. *J. Am. Chem. Soc.* **2001**, *123*, 2917−2918.
(10) Bernhard, W. A. *J. Phys. Chem.* **1989**, *93*, 2187−9.
(11) Bernhard, W. A. *Free Radical Res. Commun.* **1989**, *6*, 93−94.
(12) Cullis, P. M.; Evans, P.; Malone, M. E. *Chem. Commun.* **1996**, 985−986.
(13) Debije, M. G.; Bernhard, W. A. *J. Phys. Chem. B* **2000**, *104*, 7845−7851.
(14) Bernhard, W. A.; Mroczka, N.; Barnes, J. *Int. J. Radiat. Biol.* **1994**, *66*, 491−7.
(15) Mroczka, N. E.; Bernhard, W. A. *Radiat. Res.* **1995**, *144*, 251−7.
(16) Weiland, B.; Hüttermann, J. *Int. J. Radiat. Biol.* **1998**, *74*, 341−58.
(17) Bernhard, W. A.; Debije, M. G.; Milano, M. T.; Razskazovskiy, Y. "Influence of structure on electron and hole transfer in directly ionized DNA"; Eleventh International Congress of Radiation Research, 2000, Dublin, Ireland.
(18) Steenken, S. *Free Radical Res. Commun.* **1992**, *16*, 349−79.
(19) Wang, W.; Sevilla, M. D. *Radiat. Res.* **1994**, *138*, 9−17.
(20) Yan, M.; Becker, D.; Summerfield, S.; Renke, P.; Sevilla, M. D. *J. Phys. Chem.* **1992**, *96*, 1983−9.
(21) Gatzweiler, W.; Hüttermann, J.; Rupprecht, A. *Radiat. Res.* **1994**, *138*, 151−64.
(22) Debije, M. G.; Close, D. M.; Bernhard, W. A. *Radiat. Res.* in press.
(23) Debije, M. G.; Bernhard, W. A. *Radiat. Res.* **1999**, *152*, 583−589.
(24) Sadasivan, C.; Gautham, N. *J. Mol. Biol.* **1995**, *248*, 918−930.
(25) Tippin, D. B.; Sundaralingam, M. *Acta Crystallogr.* **1996**, *D52*, 997−1003.
(26) Bingman, C.; Li, X.; Zon, G.; Sundaralingam, M. *Biochemistry* **1992**, *31*, 12803−12812.
(27) Shui, X.; McFail-Isom, L.; Hu, G. G.; Williams, L. D. *Biochemistry* **1998**, *37*, 8341−8355.
(28) Debije, M. G.; Strickler, M. D.; Bernhard, W. A. *Radiat. Res.* **2000**, *154*, 163−170.

(29) Mercer, K. R.; Bernhard, W. A. *J. Magn. Reson.* **1987**, *74*, 66−71.
(30) Fouse, G. W.; Bernhard, W. A. *J. Magn. Reson.* **1978**, *32*, 191−8.
(31) Bernhard, W. A.; Fouse, G. W. *J. Magn. Reson.* **1989**, *82*, 156−62.
(32) Pruden, B.; Snipes, W.; Gordy, W. *Proc. Natl. Acad. Sci. U.S.A.* **1965**, *53*, 917−24.
(33) Sevilla, M. D.; Van Paemel, C.; Zorman, G. *J. Phys. Chem.* **1972**, *76*, 3577−3582.
(34) Henriksen, T. *Radiat. Res* **1969**, *40*, 11−25.
(35) Hüttermann, J. *Int. J. Radiat. Biol.* **1970**, *17*, 249−59.
(36) Spalletta, R. A.; Bernhard, W. A. *Radiat. Res.* **1993**, *133*, 143−50.
(37) Box, H. C.; Budzinski, E. E.; Potter, W. R. *J. Chem. Phys.* **1974**, *61*, 1136−9.
(38) Hole, E. O.; Nelson, W. H.; Sagstuen, E.; Close, D. M. *Radiat. Res.* **1998**, *149*, 109−119.
(39) Rustgi, S. N.; Box, H. C. *J. Chem. Phys.* **1974**, *60*, 3343−4.
(40) Polverelli, M.; Teoule, R. *Z. Naturforsch.* **1974**, *Teil C 29*, 16−18.
(41) Stetter, M.; Maulwurf, M.; Mueller, A. *Mol. Phys* **1991**, *72*, 607−18.
(42) Steenken, S.; Telo, J. P.; Novais, H. M.; Candeias, L. P. *J. Am. Chem. Soc.* **1992**, *114*, 4701−9.
(43) Hole, E. O.; Sagstuen, E.; Nelson, W. H.; Close, D. M. *J. Phys. Chem.* **1991**, *95*, 1494−503.
(44) Sagstuen, E.; Hole, E. O.; Nelson, W. H.; Close, D. M. *J. Phys. Chem.* **1992**, *96*, 1121−6.
(45) Sagstuen, E.; Hole, E. O.; Nelson, W. H.; Close, D. M. *Radiat. Res.* **1996**, *146*, 425−435.
(46) Cullis, P. M.; Malone, M. E.; Merson-Davies, L. A. *J. Am. Chem. Soc.* **1996**, *118*, 2775−81.
(47) Kar, L.; Bernhard, W. A. *Radiat. Res.* **1983**, *93*, 232−53.
(48) Bernhard, W. A. Initial sites of one-electron attachment in DNA. In *The Early Effects of Radiation on DNA*; Fielden, E. M., O'Neill, P., Eds.; Springer-Verlag: Berlin, 1991; Vol. Ser. H 54, pp 141−54.
(49) Lee, J. Y.; Bernhard, W. A. *Radiat. Res.* **1981**, *86*, 287−93.
(50) Razskazovskiy, Y.; Debije, M. G.; Bernhard, W. A. *Radiat. Res.* **2000**, *153*, 436−441.
(51) Steenken, S. *Biol. Chem.* **1997**, *378*, 1293−1297.
(52) Colson, A. O.; Besler, B.; Sevilla, M. D. *J. Phys. Chem.* **1992**, *96*, 9787−94.
(53) Colson, A. O.; Besler, B.; Close, D. M.; Sevilla, M. D. *J. Phys. Chem.* **1992**, *96*, 661−8.
(54) Wang, W.; Yan, M.; Becker, D.; Sevilla, M. D. *Radiat. Res.* **1994**, *137*, 2−10.
(55) Debije, M. G.; Milano, M. T.; Bernhard, W. A. *Angew. Chem., Int. Ed. Engl.* **1999**, *38*, 2752−2756.